ICROS-SICE International Joint Conference 2009
August 18-21, 2009, Fukuoka International Congress Center, Japan

Fastest Guidance Control Avoiding Slipping of Carrying Objects and Experimental Evaluation

Masanori Mukono[1] and Mamoru Minami[2]

[1]Graduate school of Engineering, University of Fukui, Bunkyo3-9-1, Fukui, Japan
(Tel : +81-776-27-8527;Email: mukono@rc.his.u-fukui.ac.jp)
[2]Faculty of Engineering, University of Fukui, Bunkyo3-9-1, Fukui, Japan
(Tel,Fax: +81-776-27-8527; E-mail: minami@rc.his.u-fukui.ac.jp)

Abstract: Force and torque induced by traveling motion of a mobile robot effect dynamically to the objects being carried on it. If the induced force and torque should be bigger than the static friction force and torque exerting between the carrying objects and the mobile robot, the carrying objects start to slip. Since this slipping motion causes increasing the acceleration of the mobile robot, then the slipping of one object leads to dangerous collapse of all carrying objects. Furthermore it interferes with accurate traveling motions. On the other hand, mobile robots are desired to transfer the carrying objects as fast as it can. On this view point of contradicted requirements, this paper purposes a controller to guide the mobile robot along a given course as fast as possible with acceleration restriction to avoid slipping of carrying objects during traveling.

Keywords: Mobile Robot, Carrying Object, Slipping, Guidance Method

1. INTRODUCTION

Robots have played an important role in various kinds of factories in recent years, including conveyance task of mobile robots. Force and torque induced by the traveling motion of the mobile robot dynamically affect the objects being carried on it. If the induced inertia force and torque should be larger than the maximum static friction force and torque, the carrying objects begin slipping motion on the mobile robot. The slipping of an object causes other object's slipping through increased acceleration of the mobile robot induced by the first object's slipping, resulting in bursting slipping of all carrying objects. Since the sudden change of the inertia load stemming from burst slipping influences the traveling motion as turbulence, it may cause unstable traveling, leading to accidents. From the above points, slipping motion of carrying objects and should be prevented.

We modeled motion of the mobile robot carrying object to analyze the dynamical influence of the slipping to the traveling motion based on the Newton-Eular formulation, and we conducted simulations and real experiments[1][2]. Based on the analyses of dynamical effects of slipping, we proposed a guidance control method of mobile robot to arbitrarily desired course with acceleration restriction to prevent the carrying objects from slipping[3]. This method is that maximum acceleration to prevent the carrying objects from slipping is calculated online while keeping the mobile robot travel as fast as possible and track the predesignated course as precise as possible. The effects of the proposed guidance control method such as relations of guidance parameters to trajectory-tracking accuracy, have been confirmed through several experiments and simulations.

2. NON-HOLONOMIC CHARACTER

We will call the mobile robot as link 0 in the following discussion. Fig.1 shows a frame model of a PWS mobile robot. We assumed the following as conditions for modeling the mobile robot, (1) the traveling road is flat, (2) wheels do not slip, and (3) the table to carry objects is flat. The origin of frame $\mathbf{\Sigma}_0$ that represents link 0 is set as shown in Fig.1. Since rotational motions around ${}^W\boldsymbol{x}_0$ and ${}^W\boldsymbol{y}_0$, i.e., rolling and pitching motions, are restricted geometrically by the driving wheels and the front and rear casters respectively, then angular velocity ${}^0\boldsymbol{\omega}_0$ of link 0 with respect to $\mathbf{\Sigma}_0$ is expressed as ${}^0\boldsymbol{\omega}_0 = [0\ 0\ \omega_0]^T$, $\omega_0 = \dot{\theta}_0$. Moreover, as translations in the directions of ${}^0\boldsymbol{y}_0$ and ${}^0\boldsymbol{z}_0$ are respectively restricted by the friction forces of wheels and gravity force, translation velocity ${}^0\boldsymbol{V}_0$ of link 0 with respect to $\mathbf{\Sigma}_0$ can simply expressed by ${}^0\boldsymbol{V}_0 = [V_0\ 0\ 0]^T$. Let ${}^W\boldsymbol{R}_0$ be the transformational matrix of the orientation between $\mathbf{\Sigma}_W$ and $\mathbf{\Sigma}_0$, and q_L and q_R be the rotation angle of the left and right wheels. r is radius of the left and right wheels and T means tread. Then V_0 and ω_0 are expressed as

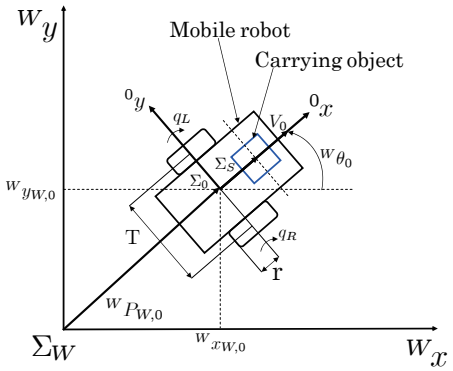

Fig. 1 Mobile robot on the standard of coordnates

$$\begin{bmatrix} V_0 \\ \omega_0 \end{bmatrix} = \begin{bmatrix} \frac{r}{2} & \frac{r}{2} \\ -\frac{r}{T} & \frac{r}{T} \end{bmatrix} \begin{bmatrix} \dot{q}_L \\ \dot{q}_R \end{bmatrix}. \quad (1)$$

Further, ${}^W\dot{x}_{W,0}$, ${}^W\dot{y}_{W,0}$, and ${}^W\dot{\theta}_0$, where ${}^Wx_{W,0}$ and ${}^Wy_{W,0}$ are the position of the origin of $\mathbf{\Sigma}_0$ in $\mathbf{\Sigma}_W$ and ${}^W\theta_0$ is the angle of link 0 around ${}^W\boldsymbol{z}_0$ in $\mathbf{\Sigma}_W$, are related to V_0 and ω_0 as

$$\begin{bmatrix} {}^W\dot{x}_{W,0} \\ {}^W\dot{y}_{W,0} \\ {}^W\dot{\theta}_0 \end{bmatrix} = \begin{bmatrix} \cos{}^W\theta_0 & 0 \\ \sin{}^W\theta_0 & 0 \\ 0 & 1 \end{bmatrix} \begin{bmatrix} V_0 \\ \omega_0 \end{bmatrix}. \quad (2)$$

By eliminating V_0 using the relations of the first and second row in the above equation, the following relation

$${}^W\dot{x}_{W,0}\sin{}^W\theta_0 - {}^W\dot{y}_{W,0}\cos{}^W\theta_0 = 0 \quad (3)$$

is obtained, which indicates that the PWS mobile robot is subjected to a lateral velocity constraint, which is non-holonomic. The Lagrange method is well known for modeling a mobile robot[4]. It requires a procedure to reduce redundant variables by using non-holonomic constraints. However, we have proposed another modeling method [5] for a mobile manipulator by expanding the Newton-Euler method used for modeling a fixed manipulator proposed by Luh[6] , which does not need a reducing process for variables. Our modeling including the slipping of carrying objects was developed based on the Newton-Euler method.

3. EXERTED FORCE

3.1 Static Friction Force

The position ${}^W\boldsymbol{P}_{W,S}$ of carrying object S in $\mathbf{\Sigma}_W$, which is being carried on the mobile robot is expressed by,

$${}^W\boldsymbol{P}_{W,S} = {}^W\boldsymbol{P}_{W,0} + {}^W\boldsymbol{R}_0\,{}^0\boldsymbol{P}_{0,S}, \quad (4)$$

where ${}^W\boldsymbol{P}_{W,0} = [{}^Wx_{W,0}, {}^Wy_{W,0}, 0]^T$, ${}^0\boldsymbol{P}_{0,S}$ is shown in Fig.1. By differentiating this by time t, ${}^W\dot{\boldsymbol{P}}_{W,S}$ and ${}^W\ddot{\boldsymbol{P}}_{W,S}$ can be represented by

$${}^W\dot{\boldsymbol{P}}_{W,S} = {}^W\dot{\boldsymbol{P}}_{W,0} + {}^W\boldsymbol{R}_0\,{}^0\dot{\boldsymbol{P}}_{0,S} + {}^W\boldsymbol{\omega}_0 \times ({}^W\boldsymbol{R}_0\,{}^0\boldsymbol{P}_{0,S}), \quad (5)$$

$${}^W\ddot{\boldsymbol{P}}_{W,S} = {}^W\ddot{\boldsymbol{P}}_{W,0} + {}^W\boldsymbol{R}_0\,{}^0\ddot{\boldsymbol{P}}_{0,S} + 2{}^W\boldsymbol{\omega}_0 \times ({}^W\boldsymbol{R}_0\,{}^0\dot{\boldsymbol{P}}_{0,S}) + {}^W\dot{\boldsymbol{\omega}}_0 \times ({}^W\boldsymbol{R}_0\,{}^0\boldsymbol{P}_{0,S}) + {}^W\boldsymbol{\omega}_0 \times \{{}^W\boldsymbol{\omega}_0 \times ({}^W\boldsymbol{R}_0\,{}^0\boldsymbol{P}_{0,S})\}. \quad (6)$$

where "$\times$" denotes the crossproduct.

The angular velocity and angular acceleration of the carrying object are

$${}^W\boldsymbol{\omega}_S = {}^W\boldsymbol{\omega}_0 + {}^W\boldsymbol{R}_0\,{}^0\boldsymbol{\omega}_S \quad (7)$$

$${}^W\dot{\boldsymbol{\omega}}_S = {}^W\dot{\boldsymbol{\omega}}_0 + {}^W\boldsymbol{R}_0\,{}^0\dot{\boldsymbol{\omega}}_S + {}^W\boldsymbol{\omega}_0 \times ({}^W\boldsymbol{R}_0\,{}^0\boldsymbol{\omega}_S). \quad (8)$$

Provided that the carrying objects are not slipping while the mobile robot is traveling, the condition is represented as ${}^0\dot{\boldsymbol{P}}_{0,S} = {}^0\ddot{\boldsymbol{P}}_{0,S} = {}^0\boldsymbol{\omega}_S = {}^0\dot{\boldsymbol{\omega}}_S = \mathbf{0}$. Substituting this condition into Eqs. (5)-(8), the object's velocity, acceleration, angular velocity, and angular acceleration given purely by the motion of the mobile robot are

$${}^W\dot{\boldsymbol{P}}^*_{W,S} = {}^W\dot{\boldsymbol{P}}_{W,0} + {}^W\boldsymbol{\omega}_0 \times ({}^W\boldsymbol{R}_0\,{}^0\boldsymbol{P}_{0,S}), \quad (9)$$

$${}^W\ddot{\boldsymbol{P}}^*_{W,S} = {}^W\ddot{\boldsymbol{P}}_{W,0} + {}^W\dot{\boldsymbol{\omega}}_0 \times ({}^W\boldsymbol{R}_0\,{}^0\boldsymbol{P}_{0,S}) + {}^W\boldsymbol{\omega}_0 \times \{{}^W\boldsymbol{\omega}_0 \times ({}^W\boldsymbol{R}_0\,{}^0\boldsymbol{P}_{0,S})\}, \quad (10)$$

$${}^W\boldsymbol{\omega}^*_S = {}^W\boldsymbol{\omega}_0, \quad (11)$$

$${}^W\dot{\boldsymbol{\omega}}^*_S = {}^W\dot{\boldsymbol{\omega}}_0. \quad (12)$$

These equations represent velocity, acceleration, angular velocity, and angular acceleration that the mobile robot gives to the carrying objects. When the object is not slipping, static friction force is balanced with inertial force, therefore static friction force ${}^W\boldsymbol{f}^*_S$ and torque ${}^W\boldsymbol{\tau}^*_S$ are given by using the above relations as

$${}^W\boldsymbol{f}^*_S = m_S\,{}^W\ddot{\boldsymbol{P}}^*_{W,S} \quad (13)$$

$${}^W\boldsymbol{\tau}^*_S = {}^W\boldsymbol{I}_S\,{}^W\dot{\boldsymbol{\omega}}^*_S + {}^W\boldsymbol{\omega}^*_S \times ({}^W\boldsymbol{I}_S\,{}^W\boldsymbol{\omega}^*_S). \quad (14)$$

However, as the value of ${}^W\boldsymbol{f}^*_S$ and ${}^W\boldsymbol{\tau}^*_S$ are limited by their maximum values, which will be discussed in the next section, it turns out that when the inertial force and torque exceeded their maximums, the carrying objects begin to slip.

Furthermore, considering a situation where p pieces are slipping within m pieces of the carrying objects, then $q(= m-p)$ pieces are still stationary. Given the k-th stationary object in q objects on link 0, and referring directly Eqs. (13) and (14), static friction forces ${}^W\boldsymbol{f}^*_{S_k}$ and ${}^W\boldsymbol{\tau}^*_{S_k}$ exerted on the k-th object are

$${}^W\boldsymbol{f}^*_{S_k} = m_{S_k}\,{}^W\ddot{\boldsymbol{P}}^*_{W,S_k} \quad (15)$$

$${}^W\boldsymbol{\tau}^*_{S_k} = {}^W\boldsymbol{I}_{S_k}\,{}^W\dot{\boldsymbol{\omega}}^*_{S_k} + {}^W\boldsymbol{\omega}^*_{S_k} \times ({}^W\boldsymbol{I}_{S_k}\,{}^W\boldsymbol{\omega}^*_{S_k}). \quad (16)$$

3.2 Maximum Static Friction Force

The maximum static friction force and torques ${}^W\boldsymbol{f}_{S,max}$ and ${}^W\boldsymbol{\tau}_{S,max}$ of the carrying object are expressed as

$${}^W\boldsymbol{f}_{S,max} = -\frac{{}^W\boldsymbol{f}^*_S}{|{}^W\boldsymbol{f}^*_S|}\mu m_S g \quad (17)$$

$${}^W\boldsymbol{\tau}_{S,max} = -[0, 0, \int_S \Delta f_S r_S ds]^T \triangleq [0, 0, \gamma_S]^T, \quad (18)$$

where, ${}^W\boldsymbol{f}^*_S/|{}^W\boldsymbol{f}^*_S|$ is the direction in which static friction is exerted, μ the static friction coefficient, m_S mass of carrying object and g is the gravity acceleration. Here, r_S is the distance from the center of the object to an infinitesimal area ds and Δf_S is the static friction force exerted at ds. As long as $|{}^W\boldsymbol{f}^*_S| < |{}^W\boldsymbol{f}_{S,max}|$ and $|{}^W\boldsymbol{\tau}^*_S| < |{}^W\boldsymbol{\tau}_{S,max}|$ hold, the object carried on link 0 is stationary without slipping.

3.3 Solid Friction Force

From the moment $|{}^W\boldsymbol{f}^*_S| > |{}^W\boldsymbol{f}_{S,max}|$ or $|{}^W\boldsymbol{\tau}^*_S| > |{}^W\boldsymbol{\tau}_{S,max}|$ is satisfied, the carrying object begins slipping in translation or rotation. The dynamical friction force and torque, ${}^W\boldsymbol{f}^{\#}_S$ and ${}^W\boldsymbol{\tau}^{\#}_S$ in Σ_W are represented by referring to solid friction as follows,

$${}^W\boldsymbol{f}^{\#}_S = -{}^W\boldsymbol{R}_0(\frac{{}^0\dot{\boldsymbol{P}}_{0,S}}{|{}^0\dot{\boldsymbol{P}}_{0,S}|}\mu' m_S g) \quad (19)$$

$${}^W\boldsymbol{\tau}^{\#}_S = -[0, 0, \int_S \Delta f_m r_S ds]^T = -[0, 0, \gamma_{sm}]^T, \quad (20)$$

where ${}^0\dot{\boldsymbol{P}}_{0,S}/|{}^0\dot{\boldsymbol{P}}_{0,S}|$ is the unit vector indicating the slipping direction, μ' is the coefficient of solid friction, and Δf_m is the solid friction force exerted on ds. Solid friction is sometimes approximated as Coulomb friction.

4. GUIDANCE METHOD

In this section, a guidance control with acceleration restriction of PWS mobile robot is proposed.

We can assume that a desired course $y_d(t) = f(x_d(t))$ is given by some trajectory planning. The position of the mobile robot in world coordinates fixed on the floor was represented by $({}^W x_0(t), {}^W y_0(t))$. And assuming position can be measured by some method like dead-reckoning, we can use $P_t({}^W x_0(t), {}^W y_0(t))$ and ${}^W\theta_0(t)$ as the value that we can use for the feedback state variables of guidance control as shown in Fig.2. Based on the current position $({}^W x_0(t), {}^W y_0(t))$ of the mobile robot, point $D_t({}^W x_t(t), {}^W y_t(t)) \triangleq ({}^W x_0(t)+L, f({}^W x_0(t)+L))$ is determined temporarily as a guidance target on the target course, where L is a position constant value chosen by referring the space frequency of the course.

The above relations are depicted in Fig.2. The calculation of the target point D_t assumes the relation that the direction of the course looks to positive direction of the x axis. However, since we can change any geometrical relations of the mobile robot and the course into such situation represented by Fig.2 by using coordinate transformation, the above assumption does not mean any restriction of the generality of this guidance method.

A circle can be determined uniquely, which passes through current position $P_t({}^W x_0(t), {}^W y_0(t))$ of the mobile robot and D_t, and tangent to ${}^W\theta_0(t)$ at P_t. Consequently the center position of the circle $C_t({}^W x_c(t), {}^W y_c(t))$ and the radius $r_c(t)$ are determined uniquely, depending on P_t, D_t, and ${}^W\theta_0(t)$. The circle is used for the instantaneous traveling trajectory from current time t to $t + \Delta t$. To let the mobile robot travel on this circle, the desired velocity V_{0d} for future period of t to $t+\Delta t$ and desired angular velocity ω_{0d} must have a relation, that is $r_c\omega_{0d} = V_{0d}$. Here in this paper V_{0d} is used for acceleration control from the start point, then V_{0d} is a depending value determined by the acceleration restriction not to slip the carrying objects, which is discussed in the following section. So ω_{0d} is got by,

$$\omega_{0d}(t) = \frac{V_{0d}(t)}{r_c(t)}. \tag{21}$$

Using ω_{0d} the desired velocity of left and right wheels V_{Ld}, V_{Rd} are calculated as follows,

$$V_{ref,i}(t) = (r_c \pm \frac{T}{2})\omega_{0d} = \frac{1}{r_c}(r_c \pm \frac{T}{2})V_{0d} (i = R, L). \tag{22}$$

This relation is shown in Fig.4. At the next control period, new target point is determined using new current position and orientation, then new instantaneous circle from the time $t + \Delta t$ to $t + 2\Delta t$ is drawn. The guidance trajectory made by connected small arcs of instantaneous traveling can be depicted as shown in Fig.3, where suffix t of P means current time t, $t + 1$ means $t + \Delta t$, and so on.

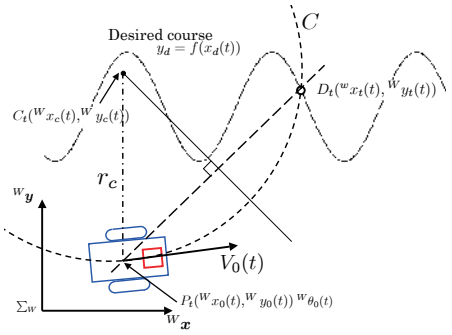

Fig. 2 Relation between the mobile robot and the target course

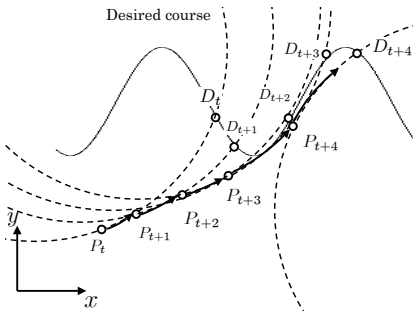

Fig. 3 Guidance method

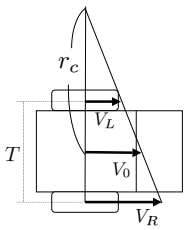

Fig. 4 Relation between $r_c(t)$ and velocity of wheels

5. ACCELERATOIN LIMITATION

5.1 Limitation of Acceleration

The acceleration is limited by using maximum static friction force ${}^W f_{S,max}$ as follows,

$$\begin{aligned} |{}^W\ddot{\boldsymbol{P}}^*_{Sk}| &= \sqrt{(\dot{V}_0 \cos\theta_0 + a_{xk})^2 + (\dot{V}_0 \sin\theta_0 + a_{yk})^2} \\ &< \frac{|{}^W\boldsymbol{f}_{S,max}|}{m_S} = \frac{{}^W f_{S,max}}{m_S}. \end{aligned} \tag{23}$$

From the above relation, we have an inequality condition to prevent objects slipping as,

$$\dot{V}_{0,min} \le \dot{V}_0 \le \dot{V}_{0,max}. \tag{24}$$

From Eq.(23) the two limitations of maximum and minimum accelerations are calculated as $\dot{V}_{0,max}$ and $\dot{V}_{0,min}$

$$\begin{matrix} \dot{V}_{0,max}, \\ \dot{V}_{0,min} \end{matrix} = \frac{-(\frac{V_0 \dot{r}_c {}^0y_S}{r_c^2} - \frac{V_0 \dot{r}_c ({}^0x_S^2 + {}^0y_S^2)}{r_c^3}) \pm \sqrt{D}}{(1 - \frac{2{}^0y_S}{r_c} + \frac{{}^0x_S^2 + {}^0y_S^2}{r_c^2})}. \tag{25}$$

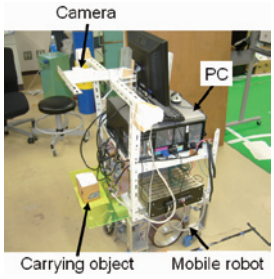

Fig. 5 Experimental system

5.2 Acceleration Restriction

The estimated acceleration in the future of one-step control period, $\dot{V}_{0d}^{+}(t)$, could be approximated as,

$$\dot{V}_{0d}^{+}(t) \fallingdotseq \frac{V_{0d}^{+}(t) - V_0^{-}(t)}{\Delta t}. \tag{26}$$

The $\dot{V}_{0d}^{+}(t)$ is compared with the maximum and minimum acceleration ($\dot{V}_{0,max}$ *and* $\dot{V}_{0,min}$), which are represented by Eq.(25). Then, if estimated acceleration is beyond the range of non-slipping extent, the exerting acceleration in the future should be limited by the following substitution,

$$\dot{\tilde{V}}_{0d}^{+}(t) = \begin{cases} \dot{V}_{0,max} - \epsilon & (\dot{V}_{0d}^{+}(t) > \dot{V}_{0,max} - \epsilon) \\ \dot{V}_{0d}^{+}(t) & \\ \quad (\dot{V}_{0,min} + \epsilon \leq \dot{V}_{0d}^{+}(t) \leq \dot{V}_{0,max} - \epsilon) & \\ \dot{V}_{0,min} + \epsilon & (\dot{V}_{0d}^{+}(t) < \dot{V}_{0,min} + \epsilon). \end{cases} \tag{27}$$

Where ϵ is a parameter to compensate the calculation accuracy of linear approximation of Eq.(26). New guidance output $\tilde{V}_{0d}^{+}(t)$ is recalculated by $\dot{\tilde{V}}_{0d}^{+}(t)$ as follows,

$$\tilde{V}_{0d}^{+}(t) = \dot{\tilde{V}}_{0d}^{+}(t)\Delta t + V_0^{-}(t). \tag{28}$$

To travel on the desired course with the newly calcurated velocity $\tilde{V}_{0d}^{+}(t)$, the desired angular velocity ω_{0d} is determined by Eq.(21) and then the desired velocities of left and right wheels $\tilde{V}_{ref,R}$, $\tilde{V}_{ref,L}$, are calculated as

$$\tilde{V}_{ref,i}^{+}(t) = (r_c \pm \frac{T}{2})\omega_{0d} = \frac{1}{r_c}(r_c \pm \frac{T}{2})\tilde{V}_{0d}^{+}(i = R, L). \tag{29}$$

6. EXPERIMENTS AND SIMULATIONS

6.1 Acceleration Restriction in the Curve Course

Traveling experiments using sinusoidal course under two kinds of situation with restricted acceleration and unrestricted acceleration are executed in order to confirm preventing effcet of not slipping. There is a photograph of the experimental system for the PWS mobile robot in Fig.5. The desired course is given as $y_d(t) = k(1 - \cos\omega x_d(t))$ as shown in Fig.6. "Slip" in Fig.6 expresses the point the carrying object begins to slip when the acceleration is not restricted. The initial position is $({}^{W}x_0(0), {}^{W}y_0(0)) = (0, 0)$ and the orientation is ${}^{W}\theta_0(0) = 0$, meaning the direction of the mobile robot equals to positive direction of x axis. The desired velocity is given by $V_{0d}(t) = \dot{V}_{0d}t[m/s]$, where $\dot{V}_{0d} = 0.03[m/s^2]$. And the initial velocity is $V_0(0) = 0$. The initial offset error of position is set as zero in x and y coordinates, and orientation error is also zero. The value of ϵ is set as 0.1 to make experiment stable. The parameter L to decide temporal target position on the course is set as $0.1[m]$. When making the mobile robot stop, $\dot{V}_{0d}$ is given as $-0.04[m/s^2]$ at $t = 8.0[s]$ in case of acceleration non-restricted experiment shown by "A" in Fig.7(a), where in this case the carrying object began to slip at $7.74[s]$, then stopping motion was set to begin at $8.0[s]$ just often the slipping. Fig.7(b) depicts the velocity profile with acceleration restriction, where the restriction has worked effectively two times and at $t = 15.5[s]$ shown by "B", the mobile robot began to stop.

The trajectories of mobile robot with and without the acceleration restriction are shown in Fig.8(a), (b). From the two trajectories, whether the acceleration restriction exerts or not does not affect the shape of the trajectories, which indicates that the acceleration restriction is independent on the guidance control since the acceleration restriction does not generate angular velocity to change heading as shown in section 5.2.

Then, shall we look at details of the results of acceleration being not restricted shown in Fig.7(a),9(a),11(a). We can find in Fig.7(a) that the mobile robot accelerates at constant acceleration until $t = 8.0[s]$. In Fig.9(a), controlled acceleration $\dot{\tilde{V}}_{0d}^{+}(t)$ exceeds maximum acceleration $\dot{V}_{0,max}$ at $t = 7.74[s]$. As a result, the carrying object began to slip at $t = 7.74[s]$. We can also see the motion of slipping carrying object by photos in Fig11(a), which give close agreement with the result of Fig.9(a).

Next, we consider the results when acceleration is restricted which are shown in Fig.7(b),9(b)-11(b). In Fig.9(b), $\dot{\tilde{V}}_{0d}^{+}(t)$ decreases coherently with decreasing maximum acceleration $\dot{V}_{0,max}$ so as not to exceed $\dot{V}_{0,max}$. Then, translational velocity $V_0(t)$ decreases because $\dot{\tilde{V}}_{0d}^{+}(t)$ is minus value. Comparing Fig.9(a) with Fig.9(b), the range that $\dot{V}_{0,max}$ decreases of Fig.9(b) is bigger than the one of Fig.9(a). The reason velocities when lies on the acceleration restriction begins to work are different. Unlike the case that the acceleration is not restricted, the carrying object does not slip when the acceleration is restricted because $\dot{\tilde{V}}_{0d}^{+}(t)$ does not exceeds $\dot{V}_{0,max}$ always. Actually, in Fig11(b), we can find that carrying object is stationary on the mobile robot.

6.2 Influence of Guidance Parameter L

We confirm how parameter L stated in section 4 affects guidance control with acceleration restriction through simulations. Desired course is shown in Fig.12. The acceleration changes to minus value for a stop in $t = 11.0[s]$. Other conditions are the same as section 6.1, we execute simulation of three patterns, $L = 0.1, 0.2, 0.3[m]$.

The simulation results are shown in Fig.13-15. Comparing each result of (a), we can find that the bigger value of L makes, guidance accuracy worse. Thus, the bigger value of L induces, the mobile robot travels looser curve. Next, we consider each result of (b). The value of maxi-

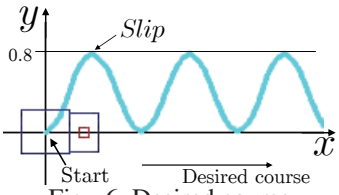

Fig. 6 Desired course

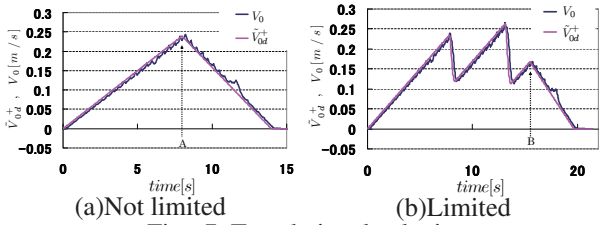

(a)Not limited (b)Limited
Fig. 7 Translational velocity

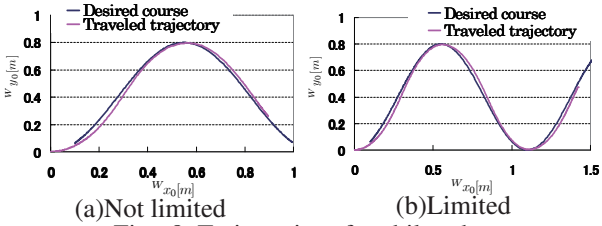

(a)Not limited (b)Limited
Fig. 8 Trajectories of mobile robot

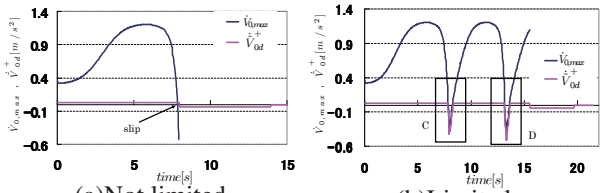

(a)Not limited (b)Limited
Fig. 9 Translational acceleration

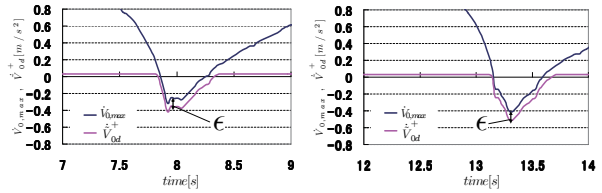

(a)Part of C for Fig.9(b) (b)Part of D for Fig.9(b)
Fig. 10 Part of Fig.9(b)

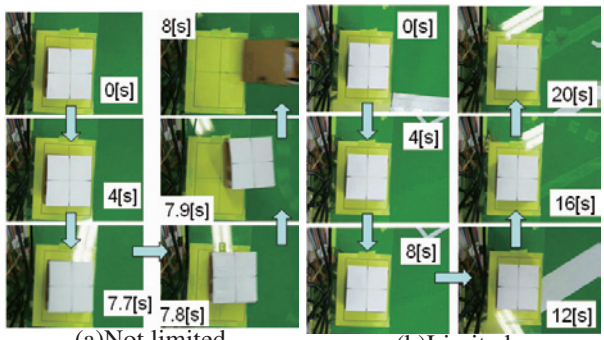

(a)Not limited (b)Limited
Fig. 11 Slipping trajectories

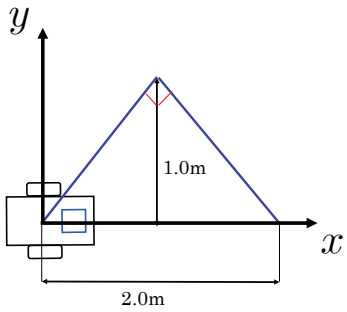

Fig. 12 Desired course

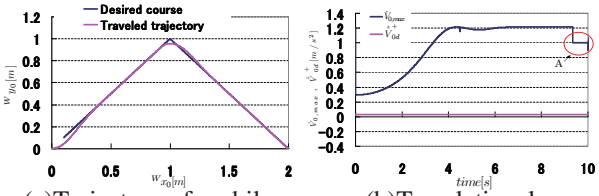

(a)Trajectory of mobile robot (b)Translational acceleration
Fig. 13 $L = 0.1$

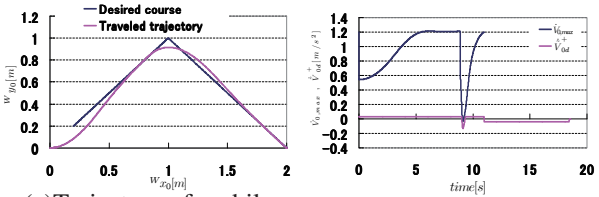

(a)Trajectory of mobile robot (b)Translational acceleration
Fig. 14 $L = 0.2$

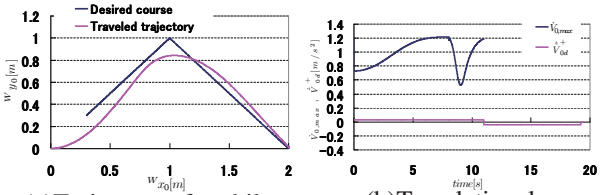

(a)Trajectory of mobile robot (b)Translational acceleration
Fig. 15 $L = 0.3$

mum acceleration $\dot{V}_{0,max}$ becomes 1.0 from $t = 9.35[s]$ shown by A in Fig.13(b). This is the reason why we set maximum acceleration $\dot{V}_{0,max} = 1.0$ when D of Eq.(25) detected to be minus. It means the maximum acceleration $\dot{V}_{0,max}$ is indeterminate from $t = 9.35[s]$. As a result, without the acceleration restriction the carrying object begins to slip. Second, in Fig.14(b), there is no part that the maximum acceleration $\dot{V}_{0,max}$ is indeterminate like as Fig.13(b), and we can find that controlled acceleration $\dot{\tilde{V}}_{0d}^+(t)$ decreases coherently with decreasing maximum acceleration $\dot{V}_{0,max}$ so as not to exceed $\dot{V}_{0,max}$ from $t = 9.03[s]$ to $t = 9.33[s]$, the acceleration is restricted. Finally, in Fig.15(b), the maximum acceleration $\dot{V}_{0,max}$ decreases, this tendency is the same as the one in Fig.14(b), but it does not reach to $\dot{\tilde{V}}_{0d}^+(t)$, so the mobile robot continued traveling without acceleration restriction.

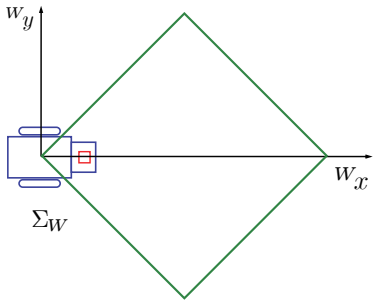

Fig. 16 Desired course (Round)

As previously mentioned, this is why the mobile robot travels looser curve than the case of $L = 0.2$.

From these results, we can say that as the value of L is bigger, the part of the maximum acceleration $\dot{V}_{0,max}$ which can not be calculated will disappear, but the guidance accuracy to desired course is worse.

6.3 Acceleration Restriction in Round Traveling

Traveling simulation using round course as shown in Fig.16 is executed in order to confirm effectiveness of the proposed method on the point of whether the proposed method can deal with continuous traveling despite the desired acceleration $\dot{V}_{0d}$ being set at positive value of $0.005[m/s^2]$. In this simulation, L is variable which depends on velocity V_0 based on results of section 6.2 , $L = 0.07 + 1.9{V_0}^2$. Other conditions are the same used in section 6.2.

The simulation results are shown in Fig.17-Fig.19. Desired course and traveled trajectory in Fig.17, maximum acceleration $\dot{V}_{0,max}$ and controlled acceleration $\dot{\tilde{V}}^{+}_{0d}(t)$ in Fig.18, and guidance control output velocity $\tilde{V}^{+}_{0d}(t)$ and translational velocity $V_0(t)$ in Fig.19 are expressed. In Fig.17, the mobile robot can follow and go round desired course. The mobile robot traveles loosely every corner because L is variable which depends on V_0. Though the proposed controller always try to increase the translational velocity, V_0 gradually saturated as shown Fig.19, thus traveled trajectory also converged. In Fig.18, $\dot{\tilde{V}}^{+}_{0d}(t)$ decreases with decreasing $\dot{V}_{0,max}$ so as not to exceed $\dot{V}_{0,max}$. We can find $V_0(t)$ decreases while the acceleration is restricted to minus value shown in Fig.19. As a result, the carrying object did not slip while the velocity was kept as high as possible and the guidance trajectory was followed to the course as accurate as possible.

7. CONCLUSION

We proposed a guidance control with acceleration restriction for mobile robot which is required to travel on arbitrary desired course as fast as possible. We confirmed the validity of the proposed method through several experiments and simulations. Influence of guidance parameter L is verified. This value should be changed suitably if the desired course is changed, therefore, there remains an open problem how to decide L.

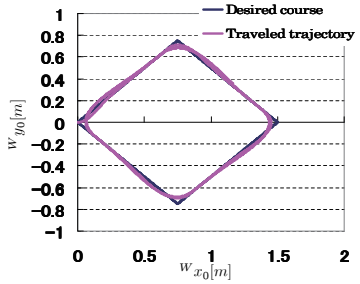

Fig. 17 Trajectory of mobile robot (Round)

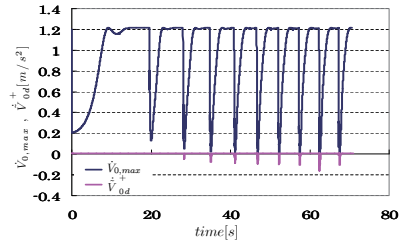

Fig. 18 Translational acceleration (Round)

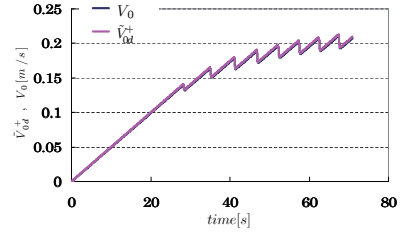

Fig. 19 Translational velocity (Round)

REFERENCES

[1] T. Ikeda, M. Takeuchi, T. Naniwa, M. Minami, Modeling of Mobile Robot Considering Slipping Movement of Carrying Objects and Experiments, *Trans. JSME*, vol. 70, no. 699, pp. 3227-3235, 2004(in Japanese).

[2] Mamoru Minami, Takeshi Ikeda and Motoya Takeuchi, Dynamical Model of Mobile Robot Including Slipping of Carrying Objects, *International Journal of Innovative Computing, Information and Control*, Vol.3, No.2, pp.353-369 (2007.4).

[3] Y. Yazaki,T. Ikeda,M. Minami,Y. Mae, Guidance Control of Mobile Robot Preventing Slipping of Carrying Objects, *Proc. The 31st Conf. of IEEE Industrial Electronics Society*, pp. 1779-1784, 2005.

[4] Fierro, R., and Lewis F. L., Control of a Nonholonimic Mobile Robot: Backstepping Kinematics into Dynamics, *J. of Robotic Systems*, vol.14, no.3, pp.149-163, 1997.

[5] M. Minami, T. Asakura, N. Fujiwara, and K. Kanbara, Inverse Dynamics Compensation Method for PWS Mobile Manipulators, *JSME Int. J.*, vol.40, no.2, pp.291-298, 1997.

[6] J. Y. S. Luh, M. Walker, and R. P. Paul, On-Line Computational Scheme for Mechanical Manipulators, *ASME Trans., J. Dynamic Systems Measurement and Control*, vol.102, pp.69-76, 1980.